Characterization of Plant Nanofiber-Reinforced Epoxy Composites

A. F. Ireana Yusra,[a] H. P. S. Abdul Khalil,[a,b,*] Md. Sohrab Hossain,[a] Yalda Davoudpour,[a] A. A. Astimar,[c] A. Zaidon,[d] Rudi Dungani,[e] and A. K. Mohd Omar [a]

In the present study, oil palm empty fruit bunch (OPEFB) fibers were taken from a 25-year-old oil palm tree. The cellulosic nanofiber (CNF) was isolated from the OPEFB using a chemo-mechanical process and utilized as reinforcement in an epoxy matrix. Various CNF loading percentages (0 to 0.75%) were applied in the epoxy matrix to explore the potential of using OPEFB-CNF as reinforcement. The morphological, mechanical, physical, and thermal characteristics of the OPEFB nanofiber-reinforced epoxy composites were evaluated. Results showed that the 0.25% and 0.5% CNF loadings were homogenously distributed and well-dispersed in the composite matrix. Conversely, agglomeration was detected in the matrix with 0.75% CNF loading. Determination of the water absorption behavior of CNF-reinforced epoxy composites at various loadings revealed that the physical properties of the composites increased with reinforcement loading. Furthermore, the analyses of the mechanical and thermal properties of the CNF-reinforced composites revealed that the incorporation of OPEFB-CNF enhanced the mechanical performance and thermal stability up to 0.5% loading.

Keywords: Epoxy; Plant fiber; Nanofiber; Nanocomposite; Mechanical properties; Thermal properties

*Contact information: a: School of Industrial Technology, Universiti Sains Malaysia, 11800 Penang, Malaysia; b: Institute of Tropical Forestry and Forest Products (INTROP) Universiti Putra Malaysia 4300 Serdang Selangor Malaysia; c: Malaysian Palm Oil Board (MPOB), Agro Product Unit, Engineering and Processing Division, 43000 Kajang, Malaysia; d: Faculty of Forestry, Universiti Putra Malaysia, Serdang, Selangor, Malaysia; e: School of Life Sciences and Technology, Institut Teknologi Bandung, Jalan Ganesha No. 10 Bandung 40132, Indonesia; *Corresponding author: akhalilhps@gmail.com*

INTRODUCTION

Plant fibers are one of the most widely used classes of materials utilized in various industries because of their outstanding properties. The main constituent of plant fibers, cellulose, particularly at the nano-size, has recently gained tremendous attention in different fields, especially to reinforce polymer composites. The term "nanocellulose-reinforced polymer composite" specifically refers to the combination of a polymer matrix with cellulose isolated at the nano-scale as reinforcement material in the polymer matrix. Research about cellulosic nanofibers as reinforcement in composites began two decades ago (Eichhorn *et al*. 2010) and was conducted because of the great stiffness of the cellulose crystal achieved by isolating single nanofibers with high crystallinity from the cellulosic source material.

In comparison to conventional composites, cellulosic nanocomposites have various advantages, such as superior thermal, barrier, and mechanical properties; better transparency; recyclability; lower weight (Abdul Khalil *et al*. 2012a,b); high flexibility; and biodegradability (Voronova *et al*. 2012). Such improvements in the characteristics of

composites can be obtained using small-diameter, superior surface area and nano-size reinforcement to increase the interaction between the constituents of the composites. They have the potential for applications in food packaging, paper, thin components in the bio-medical field, electrical and electronic devices, and others (Mathew *et al*. 2012; Yousefi *et al*. 2013).

Epoxy resin has excellent mechanical properties; high moisture, chemical and corrosion resistance; great electrical, adhesive, and thermal properties; and it undergoes little shrinkage and is therefore dimensionally stable. Its advanced properties and reasonable cost have made epoxy a polymer widely accepted in sectors such as coatings, aerospace, adhesives, semiconductors, and automotive (Pham and Marks 2002).

CNF isolated from OPEFB fibers, which are abundantly available in Malaysia, can be utilized as a reinforcing material in nanocomposites. CNF has been extensively used with a variety of polymers to produce nanocomposites (Masoodi *et al*. 2012). The available literature regarding CNF nanocomposites using epoxy resins showed that there are rare studies that have been performed on the production of epoxy nanocomposite boards reinforced with CNF fibers (Lani *et al.* 2014; Lee *et al*. 2014). However, fibril networks as reinforcement in various types of thermoset and thermoplastic polymer matrices have been explored in transparent films (Cross *et al*. 2013; Ansari *et al*. 2014). In addition, some research has promoted high-toughness nanopaper based purely on cellulosic nanofibrils (Yousefi *et al*. 2013).

Nanocomposites are typically reinforced with low percentages of nanocellulose (usually under 10%) in comparison with the high levels of filler (40% to 60%) used in conventional composites (Abdollah *et al*. 2008). To obtain the desired enhancement in the properties of the nanocomposite, CNF should be homogeneously dispersed (Lavoine *et al*. 2012) and should properly bond to the matrix. Unfortunately, there has been no prior research focused on the development and properties of OPEFB-CNF epoxy-based nanocomposite boards as a component for the automobile, packaging, and especially bio-medical industry (Abdollah *et al*. 2008; Steele *et al*. 2012; Lee *et al*. 2014).

In this study, CNF from OPEFB was used as reinforcement in the epoxy matrix to produce nanocomposite board at low reinforcement loading below 1 wt.%. The experiments were done using very low reinforcement loading to explore the applicability of the OPEFB-CNF network as reinforcement in the epoxy nanocomposite board. The morphological, mechanical, physical, and thermal characteristics of the OPEFB-CNF epoxy nanocomposite were evaluated at various reinforcement loadings. This CNF epoxy nanocomposite has the potential for applications in automotive, aerospace, and biomedical areas.

EXPERIMENTAL

Materials

Oil palm empty fruit bunch (OPEFB) fibers were taken from a 25-year-old oil palm tree obtained from the Malaysian Palm Oil Board (MPOB, Kajang, Selangor, Malaysia). The CNF was isolated from the OPEFB using a chemo-mechanical process as described elsewhere (Ireana Yusra *et al*. 2014). The details isolation process of CNF is shown in Fig. 1a. It was found that the isolated CNF have the diameter within the range 5-10 nm (Fig. 1b). CNF Later, the isolated CNF was utilized as reinforcement in the epoxy nanocomposite. Clear polymer epoxy resin (D.E.R. 331) and curing agent (A 062) were

obtained from Zarm Scientific & Supplies (Sdn. Bhd., Penang, Malaysia). Benzyl alcohol was provided by Aldrich Company (Sdn. Bhd. Penang, Malaysia).

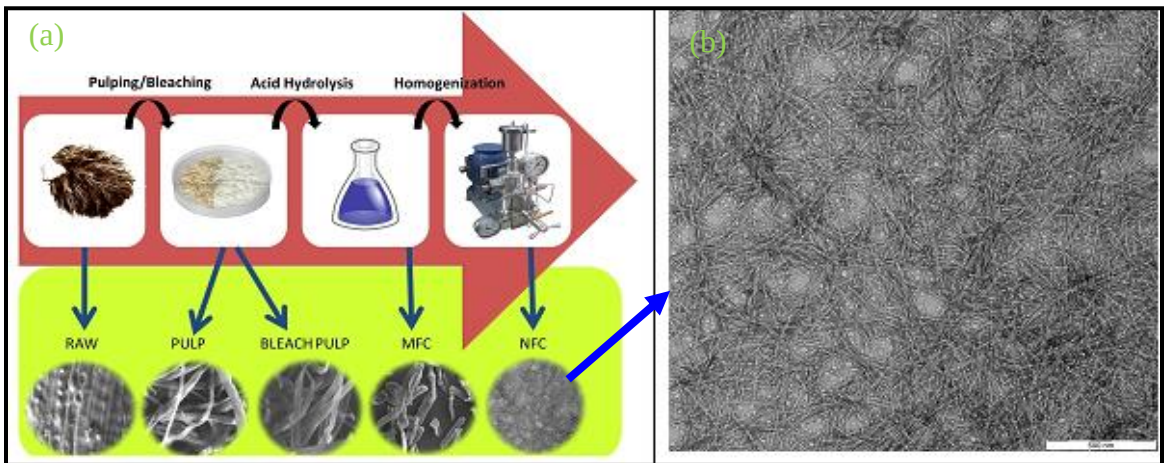

Fig. 1. (a) CNF Isolation process from the OPEFB using a chemo-mechanical process (Source: Ireana Yusra *et al*. 2014); (b) TEM image of Isolated CNF

Preparation of Nanofibrillated Cellulose Reinforced Epoxy Nanocomposites

The matrix material for all composites was prepared by mixing epoxy resin (100 phr) with the polyamide hardener (60 phr) and 10 wt.% benzyl alcohol. The nanocomposite was fabricated using low CNF reinforcement loadings of 0.25%, 0.5%, and 0.75% of the epoxy resin. A neat epoxy composite (without CNF reinforcement, 0% CNF loading) sample, as the control, was also prepared for comparison.

The desired amount of freeze-dried CNF fiber was mixed properly with the epoxy resin and 10% diluent (benzyl alcohol) for 20 min using a mechanical stirrer. Then, the polyamide curing agent was added and mechanically stirred for 10 min. The mixture was placed in a vacuum oven to eliminate the bubbles from the mixture. A 160 mm × 160 mm × 3 mm mould was sprayed with silicone oil solution as a releasing agent. The mixture was then poured into the mould and cured for 1 h at 105 °C in a hot press. After curing, the nanocomposite was post-cured in an oven for another 30 min at the same temperature. Eventually, the nanocomposite was removed from the mould and cooled at ambient temperature for 24 h prior to further analyses.

Characterization

Morphological properties

The fracture surface of the neat epoxy composite and CNF reinforced nanocomposites were observed using SEM (ZEISS EVO® MA10, Königswinter, Germany). The nanocomposite samples were retained by a SEM holder and the fracture surfaces were sputter-coated with gold (Denton Desk-1 Sputter Coater, Denton Vacuum, USA). An acceleration voltage of 15 kV was applied to capture the SEM images.

The dispersion of the CNF in the epoxy nanocomposites was studied by a transmission electron microscope (TEM, Philips CM12 instrument, Amsterdam, The Netherlands). Ultra-thin sections of a selected part of each composite sample were cut and placed on a carbon-coated grid at room temperature. Then, the samples were stained with 2% uranyl acetate and lead citrate. Images of the CNF particle distribution were captured at acceleration voltage 120 kV. The surface of the neat epoxy composite and the CNF-

reinforced nanocomposites were deposited and viewed under a light microscope at high magnification.

Physical properties

The densities of the neat epoxy composite and the CNF-reinforced nanocomposites were determined using ASTM-D1895 (1996). For each composite, five replications were utilized. Eq. (1) was employed to calculate the density of the nanocomposites,

$$\text{Density (g/cm}^3\text{)} = m / v \quad (1)$$

where m and v are the weight (g) and volume (cm^3) of the composites, respectively. All nanocomposites were weighed on a Mettler 5000 (Mettler Toledo, Malaysia) analytical balance. The volume of the samples was measured by a Mitutoyo digital veneer caliper (Mitutoyo, Malaysia).

The neat epoxy composite and the CNF-reinforced nanocomposites were immersed in water. The percentage water absorption was estimated according to ASTM D570 (2010). Samples were weighed at various time intervals. The weights of the tested nanocomposites were recorded until constant weight was obtained. Equation (2) was utilized to calculate the percentage water absorption,

$$\text{Water absorption (\%)} = \frac{W_n - W_d}{W_d} \times 100 \quad (2)$$

where W_n represents the weight of the composite after immersion and W_d is the weight of the composite before immersion.

Mechanical properties

The tensile modulus and strength of the samples was studied using an Instron 5582 test machine (USA) based on ASTM D3039 (2000). The dimensions of the samples were 120 mm × 15 mm × 3 mm. The gauge length was 60 mm and a testing speed of 5 mm/min was applied for the test.

The flexural test was performed using the three-point bending test using an Instron 5582 test machine based on ASTM D790 (2003). The crosshead speed was set at 2 mm/min. The neat epoxy composite and the CNF-reinforced nanocomposites were cut to dimensions of 160 mm × 20 mm × 3 mm.

The impact tests were conducted in a Gotech testing machine (GT-7045-MDL; China). The samples' dimensions were 70 mm × 15 mm × 3 mm based on ASTM D256 (2006).

For each sample, five repetitions were performed and the average of five tests was reported.

Thermal properties

The thermal stability of the neat epoxy composite and the CNF-reinforced nanocomposite samples were determined by thermogravimetric analysis (Perkin Elmer Pyris TGA-6, Waltham, MA, USA) and differential scanning calorimetry (DSC, Perkin Elmer DSC-821, Waltham, MA, USA). The sample was heated within the temperature ranges of 30 to 600 °C and 25 to 450 °C at heating rates of 20 and 10 °C/min in a nitrogen atmosphere for the TGA and DSC analyses, respectively.

RESULTS AND DISCUSSION

Morphological Properties

Strong interaction between CNF and polymer can be achieved through a stable, well-dispersed mixture upon the removal of flocculation and maintenance of the nanostructured scale of the substance. The strong interaction of the materials involved in nanocomposite development is determined not only by physical hydrogen bonding between nanofibrils, but also by the bonding between the CNF and polymer (Masoodi *et al*. 2012).

Light microscopy (LM) and transmittance electron microscopy (TEM) were used to illustrate and analyze the morphological properties of the nanoparticles dispersed and distributed in the nanocomposites. To view the overall dispersion and distribution of CNF in the epoxy matrix, LM images were captured and compared with varying CNF loadings from 0 to 0.75%, as presented in Fig. 2. It was observed that 0.25% and 0.5% CNF loadings were well-distributed and dispersed. Conversely, large CNF agglomeration was detected at 0.75% CNF loading (Fig. 2d), when compared with 0.25% and 0.5% CNF loadings into the nanocomposites.

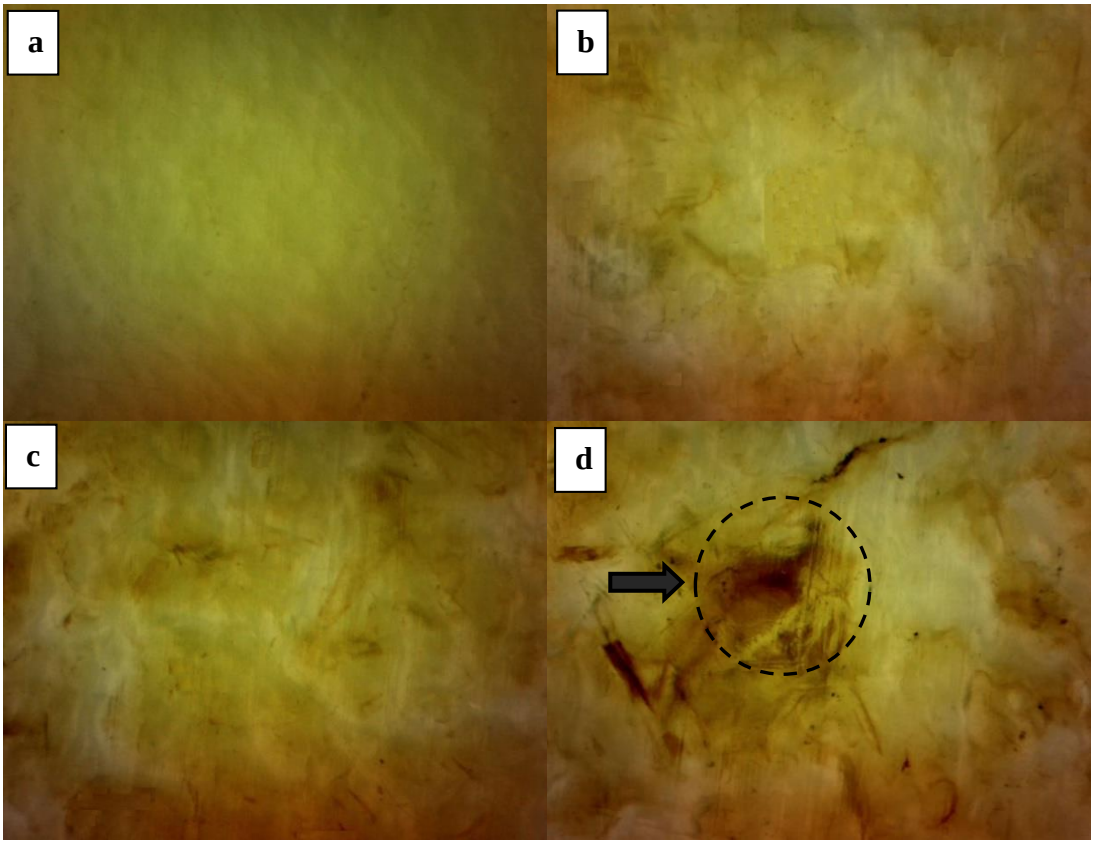

Fig. 2. Light microscopy images of CNF-reinforced epoxy nanocomposites: (a) neat epoxy, (b) 0.25% CNF, (c) 0.5% CNF, and (d) 0.75% CNF. Magnification = 100×

Figure 3 shows the TEM micrographs of the CNF-reinforced epoxy nanocomposites. It was found that CNF was homogenously dispersed in the epoxy matrix at 0.25% and 0.5% CNF loadings. Poor distribution and dispersion of CNF in the epoxy nanocomposite was observed (indicated by an arrow and dashed circle in Fig. 3c) at 0.75%

CNF loading because of the flocculation and agglomeration of nanoparticles *via* their surface functional groups (Yu *et al*. 2012). Nanocellulose has a strong tendency to agglomerate; therefore, incorporating only a low percentage of CNF is an alternative way to overcome this issue observed in both the TEM micrographs and the LM images. In addition, the large specific surface area of CNF generates a large interfacial area-per-unit volume, which can increase CNF-matrix interaction and result in better stress transfer between CNF and the matrix.

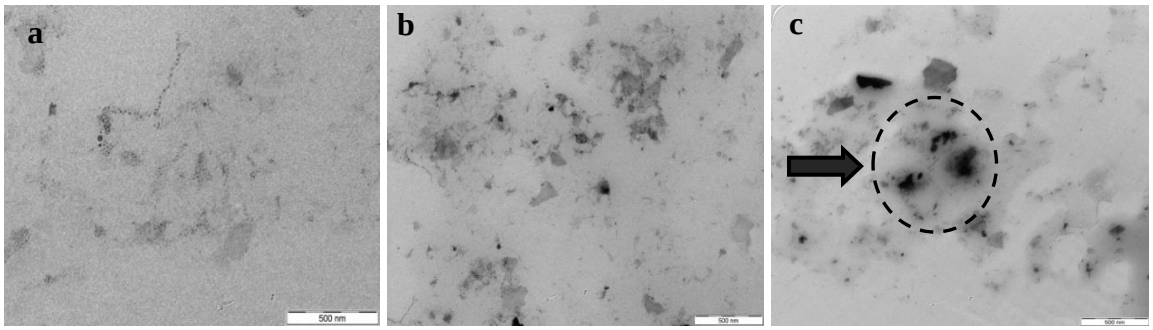

Fig. 3. TEM images of CNF loadings in epoxy nanocomposites: (a) 0.25%, (b) 0.5%, and (c) 0.75%. Magnification = 20,000 ×

SEM micrographs showing cross sections of the tensile fracture surface of the epoxy nanocomposites with 0, 0.25%, 0.5%, and 0.75% CNF loadings are shown in Fig. 4. The surface of the composite with 0% CNF loading was smooth and exhibited the brittle nature of neat epoxy composite. However, the fracture surface of the other CNF-reinforced nanocomposites was rougher. The white dots in Figs. 4b, 4c, and 4d illustrate the CNF.

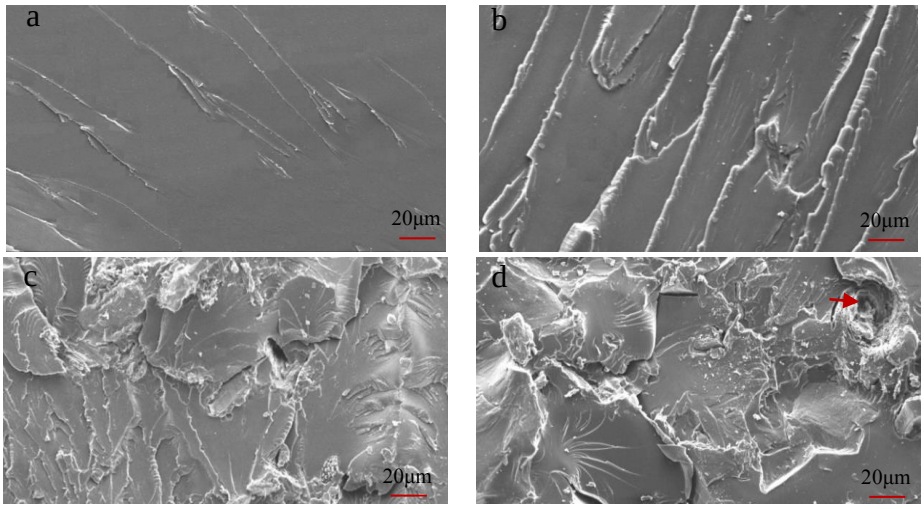

Fig. 4. SEM images of the tensile fracture surfaces of epoxy nanocomposites: (a) neat epoxy, (b) 0.25% CNF, (c) 0.5% CNF, and (d) 0.75% CNF. Magnification = 100 ×

Sharp surfaces and deep line markings were observed in the CNF-reinforced composites but not in the neat epoxy (0%) (Fig. 3a), which is evidence of the flexible fracture of the CNF added to the nanocomposite. Comparing the CNF-reinforced nanocomposites, the 0.25% CNF loading fracture surface appeared ductile (Fig. 4b).

However, the fracture surfaces at 0.5% and 0.75% CNF loadings exhibited rapid crack propagation, indicating that the cracks took more tortuous paths to disperse CNF in the nanocomposites. Thus, there was no "river line" marking observed. The difference between these two nanocomposites was the absence of agglomeration on the fracture surface micrographs of 0.5% CNF loading as compared to that of 0.75% CNF loading. This was because of the good dispersion and distribution of the CNF, without aggregation.

Further, the addition of 0.75% CNF caused little aggregation to occur (Fig. 4d). No river line markings were observed and the surface was rougher, with presence of few CNF agglomerates, as indicated by the red arrow. The presence of agglomeration was probably due to the poor dispersion and distribution of CNF in the nanocomposite. The agglomerated structure of the CNF would act as stress concentration sites under applied stress rather than the individual nanoparticles. Thus, cracks penetrated through these agglomerates, resulting in weak points and initiating failure. Hence, the aggregates were exposed on the surface (Abdul Khalil *et al*. 2013). Similarly, Abdollah *et al*. (2008) observed the smooth surface of epoxy nanocomposites with the reinforcement of low cellulose nanofiber loading (0.5 phr) as a result of adequate dispersion. Accordingly, Abdollah *et al.* (2008) reported that the fiber agglomerated at high cellulose nanofiber concentration prevented the formation of a homogeneous mixture, resulting in weak thermal and mechanical properties.

Physical Properties

The density of the CNF-reinforced epoxy nanocomposites was measured with varying CNF loading percentages. The density of the nanocomposites increased from 1.141 to 1.148 g/cm^3 at 0.25% and 0.75% CNF loadings, respectively. The density of nanocomposites increased with increasing CNF loading, perhaps because of the high density of CNF as compared to the epoxy resin. Figure 5 reveals that the percentage water absorption in the CNF-reinforced epoxy nanocomposites increased with increasing immersion times until 8 days had passed; thereafter, increases in the percentage water absorption with further immersion were negligible.

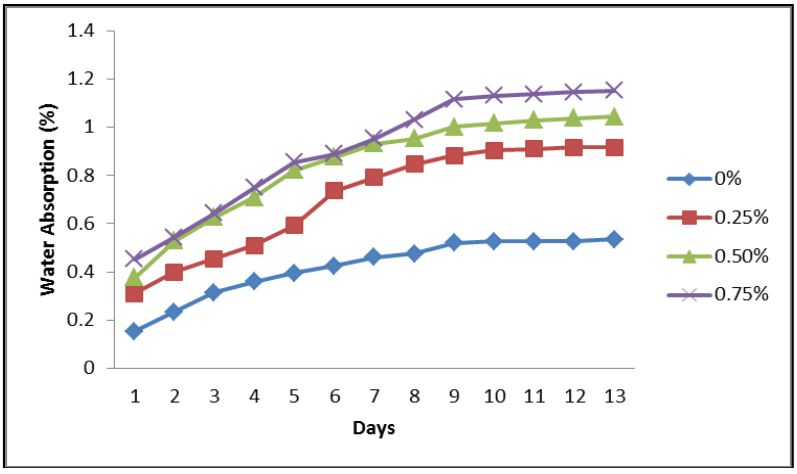

Fig. 5. Water absorption behavior of CNF-reinforced epoxy nanocomposites at various loadings

The addition of 0.75% CNF resulted in the highest percentage water absorption because of the hydrophilic nature of the composite at the highest CNF loading. This further indicated that the water absorption and weight of the nanocomposite could be related to the presence of voids and porosity in the nanocomposite. The presence of voids in

nanocomposites increases the nanocomposite weight because of water being trapped inside (Abdul Khalil *et al*. 2013). Furthermore, increased CNF loading can increase the formation of hydrogen bonds between CNF and water molecules (Lani *et al*. 2014). Abdul Khalil *et al*. (2013) reported that the percentage water absorption of polymer composites depends on the fabrication methods, the immersion time, the compositions of the composites and matrix, and the filler characteristics.

Mechanical Properties

The mechanical properties, including the tensile, flexural, and impact strengths of the CNF-reinforced epoxy nanocomposites are summarized in Table 1.

Table 1. Mechanical Properties of CNF-Reinforced Epoxy Nanocomposites

CNF Loading (%)	Tensile			Flexural		Impact (kJ/m^2)
	Strength (MPa)	Modulus (GPa)	Elongation (%)	Strength (MPa)	Modulus (GPa)	
0	23.9 ± 1.5	0.80 ± 0.6	6.95 ± 2.3	24.3 ± 1.7	1.11 ± 1.8	8.03 ± 1.9
0.25	25.1 ± 2.2	0.90 ± 0.9	5.63 ± 1.8	26.7 ± 1.4	1.17 ± 1.7	4.29 ± 1.3
0.5	27.4 ± 1.7	1.06 ± 1.1	4.08 ± 1.3	28.2 ± 1.3	1.20 ± 1.4	5.45 ± 1.6
0.75	30.1 ± 1.4	1.20 ± 1.3	3.05 ± 1.6	30.0 ± 2.0	1.25 ± 1.5	7.05 ± 1.7

The tensile strength and modulus of the nanocomposites exhibited similar increasing trends in which they increased with increasing CNF loading from 0 to 0.75%. The tensile strength and modulus of the nanocomposites ranged from 24 to 30 MPa and 0.8 to 1.2 GPa, respectively, indicating that the incorporation of CNF into the composite increased its stiffness and toughness. The maximum tensile strength and modulus of 30 MPa and 1.2 GPa, respectively, were obtained in the 0.75% CNF-reinforced nanocomposite, whereas the minimum tensile strength and modulus of 24 MPa and 0.8 GPa, respectively, were achieved in the neat epoxy nanocomposite. The increased tensile strength with CNF loading may have been because of the high surface area of CNF and good interfacial bonding between the reinforcement and the matrix, preventing quick crack propagation and improving stress transfer (Lani *et al*. 2014).

The elongation at break of the nanocomposites was reduced with increased CNF loading (Table 1). Neat epoxy (0%) had the highest elongation at break value, 6.95%, while 0.75% CNF loading reduced the elongation value to a minimum of 3.05%. The reduction in the elongation at break was probably due to fiber aggregation creating areas of stress concentrations that required less energy to propagate cracks. Pan *et al*. (2009) reported that the reduction in the elongation at break can be due to inefficient stress transfer near flaws during tensile deformation. Moreover, excess nanocellulose fiber leads increases intermolecular interaction, which might compete with the interactions between the polymer matrix and the nanocellulose fibers. Therefore, the miscibility and compatibility of the cellulose nanocomposite system was reduced, which decreased the elongation at break of the nanocomposite (Lani *et al*. 2014).

The flexural properties (strength and modulus) of the nanocomposites were found to increase with CNF loading, as shown in Table 1. This is because the small size and elevated surface area of CNF facilitate good interaction and bonding between CNF and the epoxy. The flexural strength and modulus of the samples gradually increased from 24 to 30 MPa and 1.1 to 1.3 GPa, respectively, from neat epoxy to 0.75% CNF-reinforced nanocomposite. The gradual increase in the modulus and flexural strength expose the

effective stress transfer *via* the interface. In addition, the improvement in the flexural modulus of the CNF-reinforced nanocomposites attributed to interfacial adhesion between the epoxy and the CNF dispersion such that the mobility of the chain matrix was limited with further loading (Wu *et al*. 2010).

As shown in Table 1, the impact strengths of neat resin and 0.25%, 0.5%, and 0.75% CNF-reinforced nanocomposites were 8.0, 4.3, 5.5, and 7.1 kJ/m^2, respectively. The low impact strength of the CNF-reinforced nanocomposite as compared to that of the neat epoxy was due to the low impact properties of the natural fiber. By increasing the CNF loading percentage, the impact strength changed due to the unique properties of CNF, such as its high surface area and small particle size. The findings of the present study are similar to those of a study conducted by Steele *et al*. (2012), who reported that the addition of CNF decreased the important characteristics of neat epoxy in impact testing and claimed that poor interfacial adhesion led to rapid crack propagation and reduced the impact strength. Hence, the addition of CNF can absorb energy and stop crack propagation, even at low loading percentages.

Thermal Properties

Figure 6 shows the thermal properties of the CNF-reinforced epoxy composite. The TGA analysis was carried out to determine the effect of CNF loading on the thermal stability and thermal degradation of the CNF-reinforced epoxy nanocomposites (Fig. 6a). Moreover, the maximum rate of decomposition temperature (T_{max}) was determined from the DTG curve.

From the TGA curve, all samples exhibited initial weight loss below 100 °C due to moisture loss and the evaporation of excess benzyl alcohol. The maximum degradation temperatures (T_{max}) for 0 (neat), 0.25%, 0.5%, and 0.75% CNF-reinforced were 359 °C, 435 °C, 447 °C, and 444 °C, respectively. Thus, the incorporation of CNF increased the thermal stability of the nanocomposites because of the cellulose content of the nano-reinforcement. The percentage of char residue from the non-volatile fraction is shown in Table 2. By increasing the amount of CNF loaded (0.25% and 0.5%), the char residues gradually decreased because the nanocomposite became more thermally stable and resistant to heat.

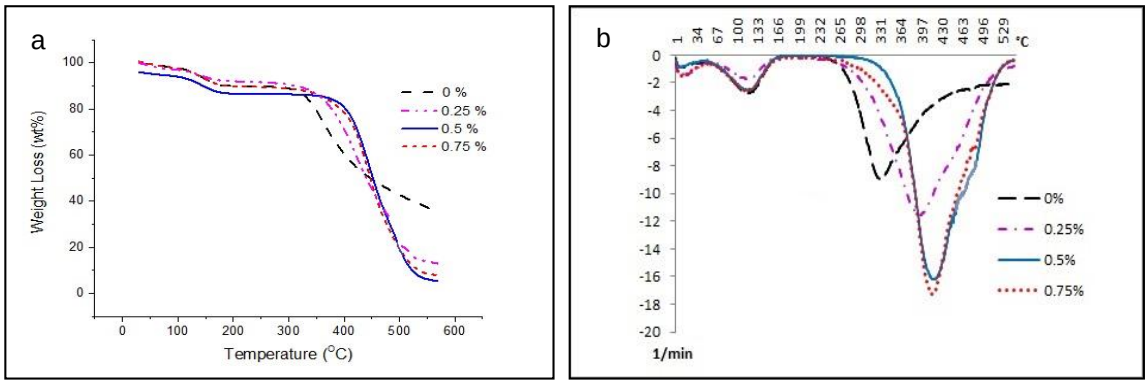

Fig. 6. Thermal properties of CNF-reinforced epoxy nanocomposites: (a) TGA curves and (b) DTG curves

Table 2. Thermal Properties of CNF-Reinforced Epoxy Nanocomposites

CNF Loading (%)	IDT (°C)	FDT (°C)	T_{max} (°C)	Residue (%)	*Melting point (°C)
0	343 ± 2.0	450 ± 1.6	359 ± 2.3	35 ± 0.3	343 ± 1.4
0.25	371 ± 2.2	535 ± 1.7	435 ± 2.0	11 ± 0.5	345 ± 1.3
0.5	406 ± 1.8	523 ± 2.1	447 ± 1.5	5 ± 0.4	362 ± 1.8
0.75	405 ± 1.3	520 ± 1.9	444 ± 1.4	8 ± 0.7	360 ± 1.6

The thermal temperatures of the nanocomposites were higher than that of neat epoxy and increased with CNF loading at 0.25% and 0.5% CNF. The increase in the thermal degradation resistance and thermal stability of nanocomposites might be due to enhanced cross-linking of the epoxy resin in the presence of CNF, minimizing particle-to-particle interaction, which shielded and consumed heat in the matrix (Cross *et al*. 2013).

At 0.75% CNF loading, a small decrease in structural destabilization was observed. This can be attributed to the agglomeration of CNF. Once nanofibers agglomerate, the interaction between fibers and fibers are stronger than those between fibers and epoxy, which may decrease the decomposition temperature due to non-limited molecular mobility (Zhou *et al*. 2012). Similar trends were also observed in the cases of IDT, FDT, and T_{max}. The results also showed that the residual weight percent of nanocomposite increased upon the addition of 0.75% CNF as a result of some inorganic residue resulting from agglomeration.

TGA analysis parameters, such as the initial decomposition temperature (IDT), final decomposition temperature (FDT), maximum temperature (T_{max}), and char residue amount, are summarized in Table 2. The melting point increased from neat epoxy to 0.5% CNF loading, at which point the biocomposites degraded at the highest temperature of 362 °C. This indicated that 0.5% CNF loading was more thermally stable, similarly to the TGA results.

The DSC curves are displayed in Fig. 7. The second endothermic of the DSC curve confirmed the TGA results as both of these analyses correspond to the decomposition and degradation of the lignin, hemicelluloses, and α-cellulose of the fiber.

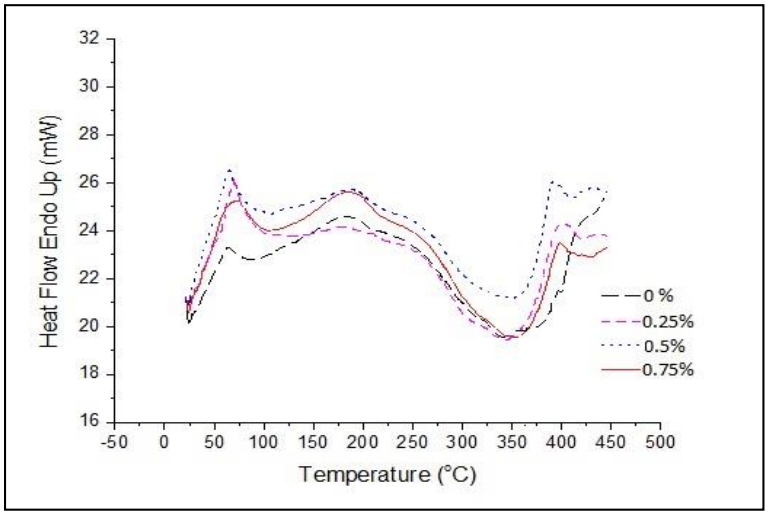

Fig. 7. DSC curves of CNF-reinforced epoxy nanocomposites

The two endothermic peaks of the CNF-reinforced epoxy-based nanocomposites were in the temperature ranges of 60 to 70 °C and 250 to 375 °C, respectively. In the first broad endothermic peak below 100 °C, the small variations in thermal energy observed were due to the evaporation of moisture.

CONCLUSIONS

1. TEM micrographs of the CNF-reinforced epoxy composites showed the homogenous dispersion of CNF in the epoxy matrix at up to 0.5% CNF loading. Poor distribution and dispersion of CNF in the epoxy composite was observed for the 0.75% CNF loading.
2. The SEM fracture surface of the neat epoxy composite was smooth and showed its brittle nature as compared to the rough surface of the CNF-reinforced composites.
3. The density of the nanocomposites increased from 1.141 to 1.148 g/cm^3 at 0.25% and 0.75% CNF loading. Thereafter, increases in the percentage water absorption with further immersion were negligible. The highest percentage water absorption was at 0.75% CNF loading.
4. The tensile and flexural properties (strength and modulus) of the nanocomposite were improved with increasing CNF loading from 0 to 0.75%. The impact strengths of the neat resin and 0.25%, 0.5%, and 0.75% CNF-reinforced composites were 8.0, 4.3, 5.5, and 7.1 kJ/m^2, respectively.
5. TGA and DSC analyses revealed the improved thermal stability of the CNF-reinforced composite as compared to that of neat epoxy.

ACKNOWLEDGEMENTS

The authors would like to thank Universiti Sains Malaysia (USM) for providing the research grants RUI:1001/PTEKIND/ 814255 and RU-PRGS: 1001/PTEKIND/846107. The authors gratefully acknowledge the Malaysia Palm Oil Board (MPOB), Malaysia for providing a research fellowship.

REFERENCES CITED

Abdollah, O., Leonardo, C. S., and Abbas, A. R. (2008). "Influences of cellulose nanofiber on the epoxy network formation," *Materials Science and Engineering A* 490(1-2), 131-137. DOI: 10.1016/j.msea.2008.01.012

Abdul Khalil, H. P. S., Bhat, A. H., and Ireana Yusra, A. F. (2012a). "Green composites from sustainable cellulose nanofibrils: A review," *Carbohydrate Polymer* 87(2), 963-979. DOI: 10.1016/j.carbpol.2011.08.078

Abdul Khalil, H. P. S., Mahayuni, R., Bhat, I. U. H., Rudi, D., Almulali, M. Z., and Abdullah, C. K. (2012b). "Characterization of various organic waste nanofillers obtained from oil palm ash," *BioResources* 7(4), 5771-5780. DOI: 10.15376/biores.7.4.5771-5780

Abdul Khalil, H. P. S., Fizree, H. M., Bhat, A. H., Jawaid, M., and Abdullah, C. K. (2013). "Development and characterization of epoxy nanocomposites based on nano structured oil palm ash," *Composites Part B: Engineering* 53, 324-333. DOI: 10.1016/j.compositesb.2013.04.013

Ansari, F., Galland, S., Johansson, M., Plummer, C. J. G., and Berglund, L. A. (2014). "Cellulose nanofiber network for moisture stable, strong and ductile biocomposites and increased epoxy curing rate," *Composites: Part A* 63, 35-44. DOI: 10.1016/j.compositesa.2014.03.017

ASTM-D1895 (1996). "Standard test methods for apparent density, bulk factor, and pourability of plastic materials," ASTM International, West Conshohocken, PA.

ASTM-D256 (2006). "Standard test methods for determining the Izod pendulum impact resistance of plastics," ASTM International, West Conshohocken, PA.

ASTM-D3039 (2000). "Standard test method for tensile properties of polymer matrix composite materials," ASTM International, West Conshohocken, PA.

ASTM-D570 (2010). "Standard test method for water absorption of plastics," ASTM International, West Conshohocken, PA.

ASTM-D790 (2003). "Standard test methods for flexural properties of unreinforced and reinforced plastics and electrical insulating materials," ASTM International, West Conshohocken, PA.

Cross, L., Schueneman, G., Mintz, E., Xu, S., Girouard, N., Shofner, M., and Meredith, C. (2013). "Nanocellulose reinforced epoxy elastomer," *Proceedings of the 36th Annual Meeting of the Adhesion*, Daytona Beach, FL.

Eichhorn, S. J., Aranguren, D. A., Marcovich, M., Capadona, N. E., Rowan, J. R., and Weder, S. J. (2010). "Review: Current international research into cellulose nanofibres and nanocomposites," *Journal of Materials Science* 45(1), 1-33. DOI: 10.1007/s10853-009-3874-0

Ireana Yusra, A. F., Abdul Khalil, H. P. S., Sohrab Hossain, Md., Astimar, A. A., Davoudpour, Y., Dungani, R., and Bhat, A. H. (2014). "Exploration of a chemo mechanical technique for the isolation of nanofibrillated cellulosic fiber from oil palm empty fruit bunch as a reinforcing agent in composites materials," *Polymers* 6(10), 2611-2624. DOI: 10.3390/polym6102611

Lani, N. S., Ngadi, N., Johari, A., and Jusoh, M. (2014). "Isolation, characterization, and application of nanocellulose from oil palm empty fruit bunch fiber as nanocomposites," *Journal of Nanomaterials* 2014, 9 pages. DOI: 10.1155/2014/702538

Lavoine, N., Desloges, I., Dufresne, A., and Bras, J. (2012). "Microfibrillated cellulose - Its barrier properties and applications in cellulosic materials: A review," *Carbohydrate Polymers* 90(2), 735-764. DOI: 10.1016/j.carbpol.2012.05.026

Lee, K. Y., Aitomäki, Y., Berglund, L. A., Oksman, K., and Bismarck, A. (2014). "On the use of nanocellulose as reinforcement in polymer matrix composites," *Composites Science and Technology* 105, 15-27. DOI: 10.1016/j.compscitech.2014.08.032

Masoodi, R., Hajjar, R. E., Pillai, K. M., and Sabo, R. (2012). "Mechanical characterization of cellulose nanofiber and bio-based epoxy composite," *Material and Design* 36, 570-576. DOI: 10.1016/j.matdes.2011.11.042

Mathew, A. P., Oksman, K., Pierron, D., and Harmand, M. F. (2012). "Fibrous cellulose nanocomposite scaffolds prepared by partial dissolution for potential use as ligament or tendon substitutes," *Carbohydrate Polymers* 87(3), 2291-2298. DOI: 10.1016/j.carbpol.2011.10.063

Pan, P., Liang, Z., Cao, A., and Inoue, Y. (2009). "Layered metal phosphonate reinforced poly(l-lactide) composites with a highly enhanced crystallization rate," *ACS Applied Materials & Interfaces* 1(2), 402-411. DOI: 10.1021/am800106f

Pham, H. Q., and Marks, M. J. (2002). "Epoxy resins," in: *Ullmann's Encyclopedia of Industrial Chemistry*, John Wiley & Sons, Hoboken, NJ. DOI: 10.1002/14356007.a09_547.pub2

Steele, J., Dong, H., Snyder, J. F., Orlicki, J. A., Reiner, R. S., and Rudie, A. W. (2012). "Nanocellulose reinforcement of transparent composites," *Proceedings of SAMPE*, Baltimore, MD, 21-24 May.

Voronova, M. I., Zakharov, A. G., Kuznetsov, O. Y., and Surov, O. V. (2012). "The effect of drying technique of nanocellulose dispersions on properties of dried materials," *Materials Letters* 68, 164-167. DOI: 10.1016/j.matlet.2011.09.115

Wu, Y., Wang, S., Zhou, D., Xing, C., Zhang, Y., and Cai, Z. (2010). "Evaluation of elastic modulus and hardness of crop stalks cell walls by nano-indentation," *Bioresource Technology* 101(8), 2867-2871. DOI: 10.1016/j.biortech.2009.10.074

Yousefi, H., Faezipour, M., Hedjazi, S., Mousavi, M. M., Azusa, Y., and Heidari, A. H. (2013). "Comparative study of paper and nanopaper properties prepared from bacterial cellulose nanofibers and fibers/ground cellulose nanofibers of canola straw," *Industrial Crops and Products* 43, 732-737. DOI: 10.1016/j.indcrop.2012.08.030

Yu, M., Yang, R., Huang, L., Cao, X., Yang, F., and Liu, D. (2012). "Preparation and characterization of bamboo nanocrystalline cellulose," *BioResources* 7(2), 1802-1812. DOI: 10.15376/biores.7.2.1802-1812

Zhou, Y. M., Fu, S. Y., Zheng, L. M., and Zhan, H. Y. (2012). "Effect of nanocellulose isolation techniques on the formation of reinforced poly (vinyl alcohol) nanocomposite films," *Express Polymer Letters* 6(10), 794-804. DOI: 10.3144/expresspolymlett.2012.85

Article submitted: June 11, 2015; Peer review completed: August 31, 2015; Revised version received and accepted: September 1, 2015; Published: October 28, 2015.
DOI: 10.15376/biores.10.4.8268-8280